Electronic Supplementary Material (ESI) for ChemComm.

Supporting Information

The effect of non-covalent conformational locks on intra-molecular charge transport

Jiang Ma, Yangyang Shi, Zhiye Wang, Xu Wang, Yunchuan Li*, Mingjun Sun, Jing Guo, Gongming Qian, Shuai Chang*

Pages:

Experimental section

General information

^{1}H NMR & ^{13}C NMR spectra were obtained on a Bruker NMR spectrometer operating at 600 and 150 MHz, respectively, in Chloroform-d using tetramethylsilane (TMS) as an internal standard. MALDI-TOF (matrix-assisted laser-desorption/ionization time-of-flight) mass spectra were performed on a Bruker BIFLEXIII TOF mass spectrometer. UV-vis absorption was done on a Shimadzu UV-2000. Cyclic voltammetry (CV) was performed on a CHI600D electrochemical workstation with a glassy carbon working electrode and a Pt wire counter electrode at a scanning rate of 0.05 V s^{-1} against a Ag/AgCl reference electrode in dichloromethane (DCM) and tetrabutylammoniumhexafluorophosphate of 0.1 mol L^{-1} as supporting electrolyte under Nitrogen bubbling. Materials: all solvents and materials were used as received from commercial suppliers. Synthetic routes of the target compounds are outlined in Scheme 1.

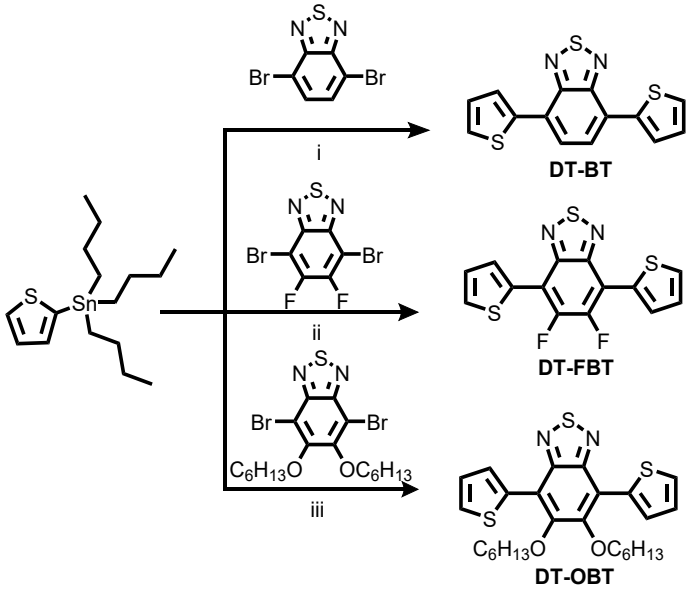

[a](i) Anhydrous toluene, 90°C, 40h, Pd(0), under N_2; (ii) DMF 120°C, 48h, Pd(0), under N_2; (iii) Anhydrous toluene,120°C, 48h, Pd(0), under N_2.

Scheme S1 Synthetic routes of DT-BT, DT-FBT, and DT-OBT.

4,7-di(thiophen-2-yl)benzo[c][1,2,5]thiadiazole (DT-BT)

DT-BT was synthesized according to the procedure described as in other's reports [1].

5,6-difluoro-4,7-di(thiophen-2-yl)benzo[c][1,2,5]thiadiazole (DT-FBT)

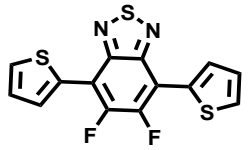

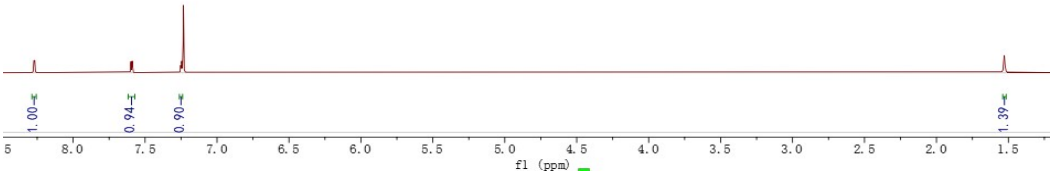

Add 5,6-difluoro-4,7-di(thiophen-2-yl)benzo[c][1,2,5]thiadiazole (0.135 mg, 0.41 mmol) and tributyl(thiophen-2-yl)stannane (0.36 mg, 0.97 mmol) into the three-necked flask. Add 20 mL of DMF and stir for 30 minutes (under N_2 atmosphere). Then $Pd(PPh_3)_4$ (67 mg) was added. After stirring for 30 minutes, it was heated to 120° C, and then refluxed for 48 hours. This mixture was poured into cold water and extracted with dichloromethane (DCM). The DCM layer was collected and dried over anhydrous $MgSO_4$. The organic solvent was distilled and the residue was purified by column chromatography using DCM: petroleum ether (1: 6) as the eluent. DT-FBT was obtained as an orange crystalline solid. ^{1}H NMR (600 MHz, Chloroform-d) δ 8.29 (s, 1H), 7.61 (d, J = 5.1 Hz, 1H), 7.26 (s, 1H), 1.55 (s, 2H). ^{13}C NMR (151 MHz, Chloroform-d) δ 150.81, 148.90, 131.52, 130.93, 130.90, 130.88, 128.91, 128.89, 128.87, 127.41, 111.71. MS (MALDI-TOF): m/z calcd for $C_{14}H_6F_2N_2S_3$ 335.97; found 335.973.

5,6-bis(hexyloxy)-4,7-di(thiophen-2-yl)benzo[c][1,2,5]thiadiazole (DT-OBT)

Add 5,6-bis(hexyloxy)-4,7-di(thiophen-2-yl)benzo[c][1,2,5]thiadiazole (0.127 mg, 0.26 mmol) and tributyl(thiophen-2-yl)stannane (0.36 mg, 0.56 mmol) into the three-necked flask. Add 20 mL of anhydrous toluene and stir for 30 minutes (under a nitrogen

atmosphere). Then $Pd(PPh_3)_4$ (60 mg) was added. After stirring for 30 minutes, it was heated to 120°C, and then refluxed for 40 hours. This mixture was poured into cold water and extracted with dichloromethane (DCM). The DCM layer was collected and dried over anhydrous $MgSO_4$. The organic solvent was distilled and the residue was purified by column chromatography using DCM: petroleum ether (1:5) as the eluent. DT-OBT was obtained as an orange oil. ^1H NMR (600 MHz, Chloroform-d) δ 8.47 (dd, J = 3.8, 1.1 Hz, 1H), 7.51 (dd, J = 5.2, 1.1 Hz, 1H), 7.23 (dd, J = 5.2, 3.8 Hz, 1H), 4.11 (t, J = 7.1 Hz, 2H), 1.94 – 1.90 (m, 2H), 1.37 – 1.30 (m, 5H), 0.92 (dd, J = 14.0, 8.4 Hz, 4H). ^{13}C NMR (151 MHz, Chloroform-d) δ 151.96, 150.99, 134.10, 130.52, 127.28, 126.73, 117.61, 31.69, 30.27, 28.25, 26.75, 25.59, 22.60, 17.27, 14.01, 13.57. MS (MALDI-TOF): m/z calcd for $C_{26}H_{32}N_2O_2S_3$ 500.16; found 500.158.

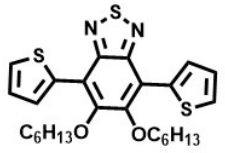

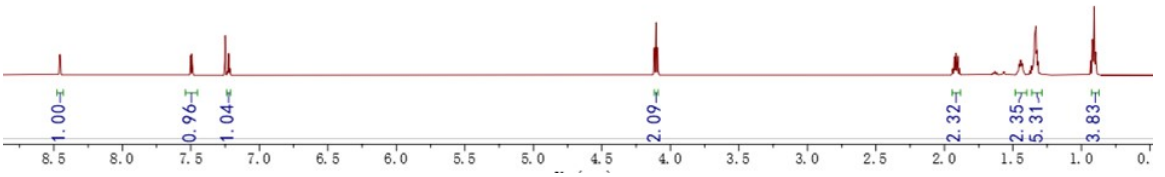

Single molecular conductance measurement

The conductance measurements were performed on an electrochemical scanning probe microscope (Agilent 6500) by adopting the Scanning tunneling microscope (STM) based recognition tunneling method. By maintaining a fixed distance between the tip and the substrate, a target molecule can be trapped in such nano gap accidentally to form a conducting loop. The target molecules were diluted to a concentration of 1mM in 1, 2, 4-trichlorobenzene (TCB) and the conductance measurements were also performed in the same solvent condition.

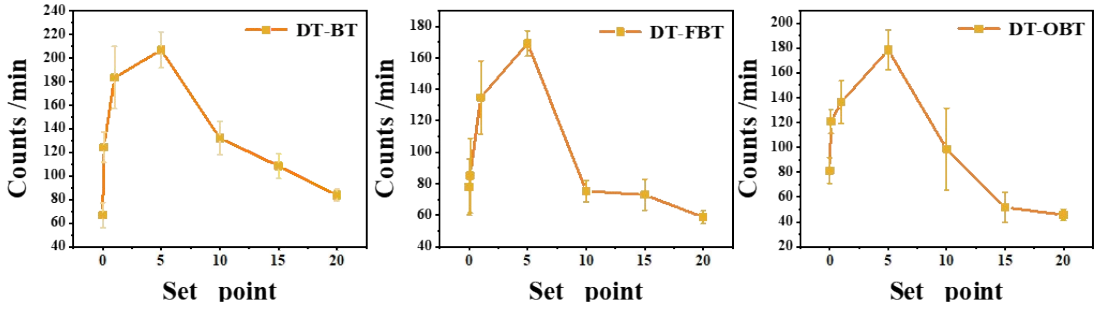

Figure S1 The signal counts of DT-BT, DT-FBT, and DT-OBT at the different set-point.

By setting different set-point (0.01, 0.1, 1, 5, 10, 15, 20 nA), the condition capable of giving the largest number of blinks per minute was determined. As shown in the Figure S1, the total blinks numbers (counts) per minutes of DT-BT, DT-FBT, and DT-OBT all peaked at 5 nA. The gap distance was then calculated based on the formula $G = G_0 * e^{(-\beta L)}$, (where $G_0 = 2e^2h^{-1}$=77.5 μS, in which e is the charge on an electron, and h is Planck's constant, β is the decay constant (6.08 nm^{-1}) for solvent 1, 2, 4-trichlorobenzene). At set-point current of 5 nA, the gap distance is about 0.83 nm. Meanwhile, the S-S distance of the optimized structures is 0.76-0.78 nm. This is close to the gap distance at 5 nA, thus conducive to junction formation.

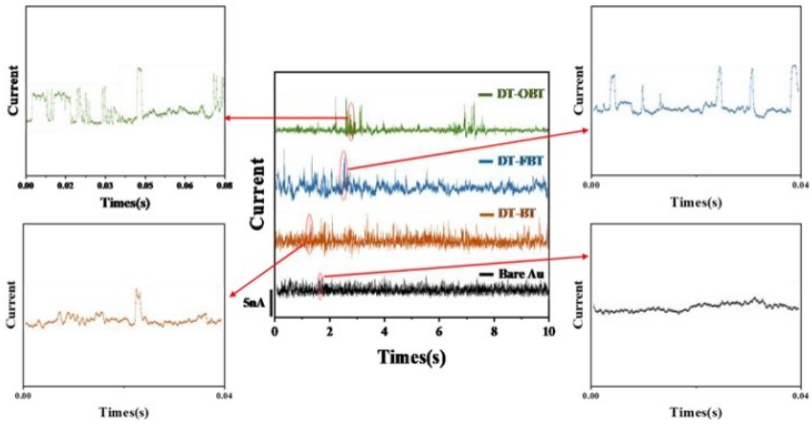

Figure S2 Typical current signal of DT-BT, DT-FBT, and DT-OBT compared with bare Au. (Typical current-time traces of target molecules and control experiment)

Typical I(t) curves were obtained in the STM measurements with a background

tunneling current of 20 nA at a bias of 0.01 V. The trace of target molecules presented lots of typical switching spikes (inset shows the details), while no identical signals were observed in control experiment.)

The repeated experiment was performed via using different Au tips or substrates which showed high reproducibility of the single molecule conductance of three molecules.

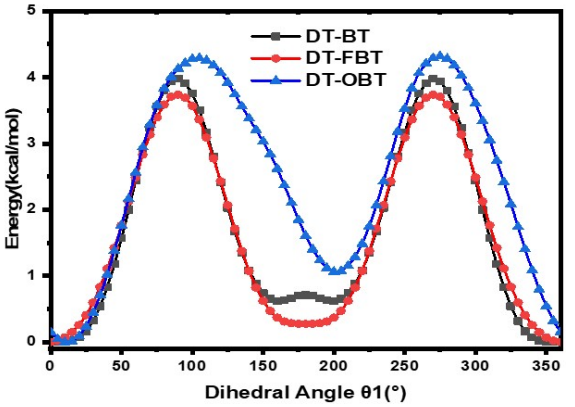

Figure S3. The molecule energy of DT-BT, DT-FBT, and DT-OBT at different dihedral angles.

In order to ensure molecular structures, the scan processes of these molecules were performed using density functional theory (DFT) at the B3LYP/6-311G* level. Dihedral angles (θ_1) between the thiophene unit and intermediate benzene ring were scanned from 0° to 360° to produce the molecule energy relative to their lowest molecule energy, as shown in Figure S4. From the energy perspective, these structures with the S atom facing down in thiophene are more stable because of non-covalent conformational locks (NCLs).

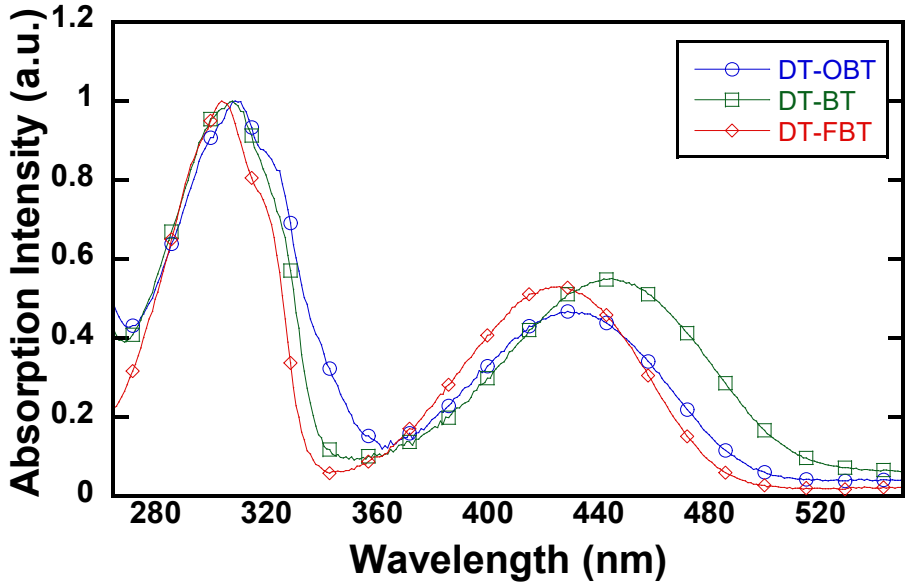

Figure S4 The absorption spectra of DT-BT, DT-FBT, and DT-OBT (10-5 M in DCM)

Electronic structure and Transport calculations

The system is calculated in the density functional theory (DFT) method. The ground state geometry of the three molecules in the gas phase was optimized using B3LYP/6-31+G* basic set. Additionally, 6-31G** and 6-311G* basis set were also used for geometries optimization whose result didn't varied much with each other. Then, the optimized structures based on *6-31+G** were inserted into two electrodes to form molecular junctions. The initial distance between the S atom of thiophene and the apex atom of each gold pyramid was 2.6 Å, with an Au–Au bond length of 2.88 Å. Figure S5 illustrates the representative model of the molecular junction with Au/molecule/Au structure. The optimized geometries and transport behaviors of the molecular junctions were studied using DFT-NEGF under the Atomistix Toolkit (ATK) package. The generalized gradient approximation (GGA-PBE) is used to calculate the electron exchange and correlation. The single zeta polarization (SZP) basis set for the Au atom, and the double zeta polarization (DZP) basis set was employed for C, H, O, N, F, and S atoms. In the optimization process, the scattering area including central organic molecule was relaxed completely, while the coordinates of the electrode atoms were frozen.

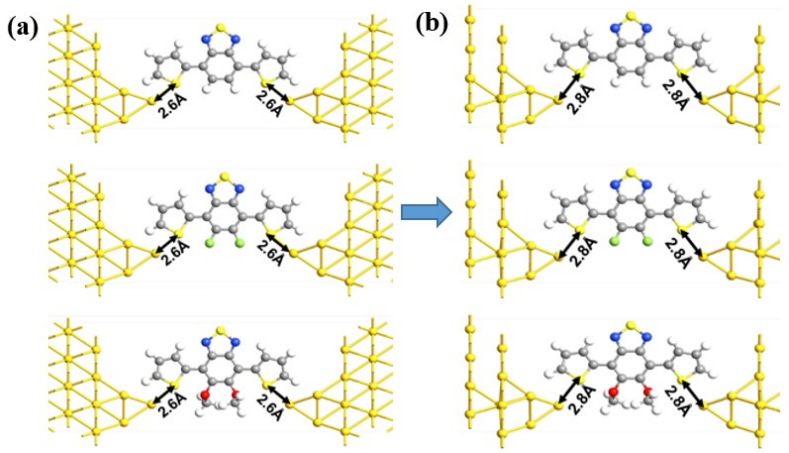

Figure S5 (a) The initial molecular junction, (b) the optimized molecular junction, while 4×4 Au atoms were used to simulate the electrodes.

According to the optimized geometries, the S-F distance is 2.88 Å and the S-O distance is 2.85 Å which are both smaller than the standard standard van der Waals radius (3.17 Å and 3.25 Å) [2]. Thus, it indicated the NCLs were conserved in the molecular junctions.

#p B3LYP/6-31(d, p) opt freq

Cartesian coordinates of DT-BT

C	-2.87204	-0.78935	-0.03917
C	-3.82116	0.21369	-0.12599
C	-5.15702	-0.25973	-0.1801
C	-5.23016	-1.6267	-0.13187
S	-3.66791	-2.35698	-0.00496
H	-3.56767	1.26703	-0.13302
H	-6.02388	0.38772	-0.24355
H	-6.11421	-2.24941	-0.14502

C	-1.42248	-0.61972	-0.01034
C	-0.77248	0.66325	-0.03837
C	-0.55874	-1.70291	0.04379
C	0.6805	0.79056	-0.03008
C	0.84996	-1.5834	0.04376
H	-0.97096	-2.70421	0.10128
C	1.52976	-0.37488	0.00641
H	1.41997	-2.50657	0.08496
N	-1.4054	1.83857	-0.07092
S	-0.25227	3.00607	-0.08829
N	1.09132	2.06275	-0.05731
C	2.98532	-0.29024	0.0111
C	3.80308	0.82228	-0.01091
S	3.97141	-1.75208	0.04791
C	5.19118	0.5122	0.0023
H	3.40451	1.8264	-0.03561
C	5.43845	-0.83236	0.03382
H	5.97365	1.26208	-0.01122
H	6.3916	-1.34225	0.04946

Cartesian coordinates of DT-FBT

C	2.91753	-0.56268	0.00002
C	3.88976	0.4265	0.00023
C	5.21599	-0.07343	0.00038
C	5.26284	-1.44173	0.00029
S	3.68757	-2.14974	0.00003

H	3.65504	1.47976	0.00025
H	6.09513	0.56028	0.00046
H	6.13553	-2.08065	0.00024
C	1.46913	-0.39601	0.00013
C	0.80697	0.88709	0.00013
C	0.57602	-1.45047	0.0003
C	-0.64636	1.03092	0.00009
C	-0.83858	-1.31308	0.00025
C	-1.52745	-0.11636	0.00007
N	1.44893	2.05381	0.0002
S	0.31182	3.23803	0.00028
N	-1.04009	2.30526	0.00021
C	-2.98058	-0.0137	-0.00018
C	-3.75128	1.13609	-0.00071
S	-4.03217	-1.43259	0.0003
C	-5.14825	0.88728	-0.00083
H	-3.31163	2.12259	-0.00101
C	-5.45008	-0.44789	-0.00033
H	-5.89636	1.67136	-0.00134
H	-6.42571	-0.91437	-0.00029
F	1.00249	-2.72586	0.00047
F	-1.50813	-2.48059	0.00032

Cartesian coordinates of DT-OBT (methyl)

C	2.95927	0.16201	-0.01345
C	3.81732	1.24236	0.10118

C	5.19271	0.89858	0.02883
C	5.39426	-0.44302	-0.14703
S	3.90537	-1.31799	-0.22251
H	3.45573	2.25187	0.2259
H	5.995	1.62348	0.10499
H	6.33335	-0.97299	-0.23271
C	1.49807	0.17145	-0.00486
C	0.73101	1.39778	-0.01367
C	0.71914	-0.97719	0.01892
C	-0.73061	1.39781	0.01315
C	-0.71882	-0.97711	-0.02009
C	-1.49769	0.17151	0.00427
N	1.25039	2.62673	-0.02507
S	0.00021	3.69037	0.0001
N	-1.24999	2.62675	0.02485
C	-2.95891	0.16218	0.01345
C	-3.81695	1.24235	-0.10271
S	-3.90492	-1.31736	0.22586
C	-5.19232	0.8988	-0.02871
H	-3.45539	2.25162	-0.22959
C	-5.39383	-0.44244	0.14988
H	-5.99462	1.6236	-0.1057
H	-6.33288	-0.97221	0.2372
O	1.33725	-2.2032	0.02018
O	-1.33666	-2.20335	-0.02194

C	1.28391	-2.91837	1.27024
H	0.25062	-3.15927	1.53013
H	1.85577	-3.83391	1.11445
H	1.74933	-2.32994	2.06774
C	-1.28747	-2.91536	-1.27385
H	-0.25488	-3.15069	-1.54161
H	-1.85356	-3.83423	-1.11661
H	-1.76105	-2.3275	-2.06696

Cartesian coordinates of DT-OBT (hexyl)

C	2.02243	2.93412	0.3113
C	3.06365	3.8065	0.06403
C	2.77126	5.15714	0.38124
C	1.51172	5.31945	0.88343
S	0.64772	3.8258	0.95716
H	4.01526	3.47486	-0.32063
H	3.47129	5.97166	0.24047
H	1.0291	6.23274	1.20083
C	2.01121	1.48113	0.1506
C	3.237	0.72317	0.08489
C	0.85885	0.719	0.05764
C	3.23681	-0.72376	-0.08509
C	0.85866	-0.71899	-0.05785
C	2.01083	-1.4814	-0.15078
N	4.4639	1.23769	0.14796
S	5.52559	-0.0006	-0.00012

N	4.46357	-1.23861	-0.14819
C	2.02171	-2.93441	-0.3114
C	3.0626	-3.80706	-0.06372
S	0.647	-3.82573	-0.95773
C	2.76996	-5.15762	-0.38099
H	4.01417	-3.47565	0.32128
C	1.51056	-5.31961	-0.88365
H	3.46972	-5.97233	-0.23993
H	1.02781	-6.23278	-1.2012
O	-0.37215	1.32104	0.10958
O	-0.3725	-1.32071	-0.10969
C	-0.99535	1.51347	-1.18978
H	-0.86511	0.60016	-1.77449
H	-0.47409	2.33283	-1.69782
C	-0.99551	-1.51311	1.18976
H	-0.86512	-0.59982	1.77445
H	-0.47423	-2.33251	1.69773
C	-2.47422	-1.81809	1.02213
H	-2.89076	-1.88527	2.03404
H	-2.95845	-0.95668	0.5495
C	-2.47401	1.81855	-1.02193
H	-2.89071	1.88573	-2.03377
H	-2.95821	0.95718	-0.54919
C	-2.79602	3.08986	-0.22929
H	-2.32352	3.95288	-0.71503

H	-2.33662	3.01277	0.75972
C	-2.79644	-3.08936	0.22951
H	-2.32397	-3.95243	0.71519
H	-2.33712	-3.01231	-0.75953
C	-4.29894	-3.35787	0.05862
H	-4.77089	-2.49172	-0.42484
H	-4.42396	-4.19214	-0.64284
C	-5.05417	-3.68939	1.35156
H	-4.55754	-4.53003	1.85283
H	-4.99673	-2.84625	2.04929
C	-6.5253	-4.03721	1.11099
H	-6.62711	-4.90734	0.45475
H	-7.04165	-4.26855	2.04685
H	-7.05867	-3.20667	0.63763
C	-4.29848	3.35854	-0.05824
H	-4.77046	2.49247	0.42535
H	-4.42333	4.19288	0.64315
C	-5.05382	3.69001	-1.35113
H	-4.55715	4.53055	-1.85254
H	-4.99653	2.8468	-2.04878
C	-6.52489	4.038	-1.11044
H	-6.62655	4.90821	-0.45429
H	-7.04131	4.26929	-2.04628
H	-7.05829	3.20756	-0.63694

[1] D. Çakal, Y. E. Ercan, A. M. Onal, A. Cihaner，*Dyes & Pigm.*, 2020,**182**, 108622

[2] H. Huang, L. Yang, A. Facchetti, T. J. Marks, *Chem. Rev.*, 2017, **117**, 10291